Insights into the mechanism of Tau amyloid assembly using anionic inducer

A

Dissertation

Submitted in partial fulfilment of the requirement for the

Degree of

Masters of Science

in

Biochemistry

By

Anjali Giri

Roll No.:301707001

Under the Supervision of

Dr. Mily Bhattacharya

(Assistant Professor)

School of Chemistry & Biochemistry
Thapar Institute of Engineering & Technology
Patiala-147004, India

15 July 2019

CERTIFICATE

This is to certify that the dissertation entitled, "**Insights into the mechanism of Tau amyloid assembly using anionic inducer**", being submitted by **Ms. Anjali Giri** in partial fulfilment of requirement for the award of the degree of **Masters of Science** in **Biochemistry** and being submitted to the School of Chemistry and Biochemistry, Thapar Institute of Engineering and Technology, Patiala is a bonafide work carried out by her under my supervision. The work has reached the standard necessary for submission, and the contents of this dissertation have not been submitted to any other university or institute for the award of any degree or diploma.

MB 06/09/19

Dr. Mily Bhattacharya
Assistant Professor
School of Chemistry and Biochemistry
Thapar Institute of Engineering and Technology, Patiala - 147004

CANDIDATE'S DECALARATION

I, hereby, declare that the work being presented in the dissertation entitled **"Insights into the mechanism of Tau amyloid assembly using anionic inducer"** in partial fulfilment of the requirement for the award of the degree of **Masters of Science** in Biochemistry and being submitted to School of Chemistry and Biochemistry, Thapar Institute of Engineering and Technology, Patiala is my own research work carried out during the period of January to July 2019 under the supervision of **Dr. Mily Bhattacharya**. I have not submitted the contents embodied in this dissertation for the award of any degree elsewhere.

Anjali Giri

Anjali Giri

Date: 6 Sep 2019

It is certified that the above statement made by the student is correct to the best of my knowledge and belief.

06/09/19

Dr. Mily Bhattacharya
Assistant Professor
School of Chemistry and Biochemistry
Thapar Institute of Engineering and Technology, Patiala - 147004

ACKNOWLEDGEMENT

I would like to express my sincere gratitude to my supervisor, **Dr. Mily Bhattacharya**, Assistant Professor, School of Chemistry and Biochemistry, Thapar Institute of Engineering and Technology, Patiala, for her relentless guidance, support and encouragement throughout this project work. It was an extremely enlightening and knowledgeable experience to work under a truly devoted person.

I am indebted to **Dr. Amjad Ali**, Head of School of Chemistry and Biochemistry and **Dr. Diptiman Choudhury**, Coordinator of MSc Biochemistry for their support throughout the programme and for giving me such a wonderful opportunity to work and pursue my interest. I would like to extend my thanks to **Dr. Amjad Ali**, **Dr. Diptiman Choudhury** and **Dr. Raj Kumar Das** for giving me permission to stay very briefly at IISER Mohali for conducting a few experiments including circular dichroism.

I express my deep sense of gratitude to **Dr. Samrat Mukhopadhyay**, Associate Professor, IISER Mohali, for allowing me to use the facilities available in his laboratory for protein expression and purification, biochemical experiments and for recording fluorescence anisotropy data. I am extremely thankful to all the research scholars of his lab especially **Ms. Aishwarya** and **Mr. Sandeep**, for all their generous help.

I am grateful to Dr. Diptiman Choudhury's lab members especially **Ms. Parmandeep Kaur**, **Ms. Vanshita Goel**, **Ms. Deepika** and **Ms. Pawan** for allowing me to use the facilities of their lab. I sincerely thank and admire the contribution of, research scholar, **Ms. Jaspreet Kaur** for helping and guiding me throughout my dissertation work like an elder sister. I am extremely thankful to her for helping me in plotting and analysing the data. I sincerely admire the contribution of my labmate, **Akanksha** for her supportive nature and for all the fun we had during our dissertation work.

I would like to thank SCBC **lab technicians** for providing me the required chemicals and facilities for this research work. I am also thankful to **SCBC staff**. I am grateful to my all classmates and friends especially **Anjali, Anushka**, **Nehal**, **Komal** and **Harmeet** for their cheerful nature and constant support throughout this programme. This journey would not be this beautiful without them.

Last but not the least, I am extremely grateful to my family members especially my parents for their constant love, support and encouragement.

Date 6 Sep 2019

Place: Patiala

Anjali Giri

Anjali Giri

TABLE OF CONTENTS

LIST OF FIGURES

LIST OF ABBREVIATIONS

ABBREVIATIONS	FULL FORMS
Aβ	Amyloid β
AD	Alzheimer's disease
AFM	Atomic force spectroscopy
CBD	Cortico basal degeneration
CD	Circular dichroism
DS	Down's syndrome
EPR	Electron paramagnetic resonance
FTIR	Fourier transform infrared spectroscopy
IDP	Intrinsically disordered protein
MT	Microtubule
NFT	Neurofibrillary tangles
NMR	Nuclear magnetic resonance
PeDB	Protein ensemble database
PHF	Paired helical filament
PiD	Pick's disease
PSP	Progressive supranuclear palsy
SDS	Sodium dodecyl sulphate
SF	Straight filaments
TAD	Transactivator domain
WT	Wild-type

ABSTRACT

Tau is a natively unfolded or an intrinsically disordered (IDP) protein which is also known to form ordered β-sheet-rich amyloid fibrils that are implicated in various neurodegenerative disorders such as frontotemporal dementia, Down's syndrome, Alzheimer's disease etc. Studies have indicated that Tau forms paired helical filaments which subsequently transform into neurofibrillary tangles that result in various tauopathies associated with declining cognition abilities. It has been demonstrated that the Tau repeat domain is the primary component of the amyloid core present in the paired helical filaments and consequently, studying the amyloid formation mechanism of tau repeat domain has generated a lot of interest over the past few years. In this research work we have mainly focused on the repeat domain of Tau i.e. Tau K18 for aggregation because it is known in literature that the repeat region of tau is more prone to aggregation. Earlier reports have revealed that tau aggregation *in vitro* is triggered by anionic inducers, however, the molecular mechanism of Tau amyloid aggregation still remains elusive. Here, we have investigated the amyloid aggregation mechanism of Tau K18 using a well-known lipid mimetic and an anionic inducer namely, sodium dodecyl sulphate (SDS) at sub-micellar concentration by spectroscopic techniques such as fluorescence and circular dichroism (CD) in addition to biochemical techniques and atomic force microscopy. Our findings indicate that TauK18 amyloid aggregation proceeds via a nucleation-dependent polymerization mechanism mediated via electrostatic interactions. Additionally, formation of a partially α-helical intermediate occurs at the initial time-points which is an aggregation-competent conformer that eventually transforms into cross β-sheet-rich amyloid fibrils.

CHAPTER 1

Introduction

Other than water, proteins are the most abundant biomolecules and our body contains approximately 100,000 distinct types of proteins, which virtually controls or stimulate all the chemical processes of our body such as catalysis, transportation, recognition etc.[1]. The central dogma is a two-step process (Fig. 1.1) by which the information is passed into the proteins from the genetic material of our body. Proteins are bio-macromolecules which are formed of one or more types of L-α-amino acids with varying side-chains that differ in terms of polarity, size, electronic structure etc. Proteins structural hierarchy shows that the different amino acids in a protein chain are joined via amide bonds and as a result give rise to the primary structure of proteins. Various non-covalent interactions such as hydrophobic interactions, van der Waals and hydrogen bonding etc., interplays within the primary structure of proteins and give rise to two different types of secondary structure, the α-helical and the β-strands and the secondary structure further lead to the formation of three-dimensional globular folded structure known as the tertiary structure. The functional diversity of proteins is governed by their tertiary structure. They work as enzymes by reducing the activation energy of various biochemical reactions, provide mechanical and immune support, store and transport molecules, transmit nerve impulse, control growth and differentiation etc. However, changes in pH, ionic strength, temperature in their cellular environment can destabilize their structure and result in loss of function [2].

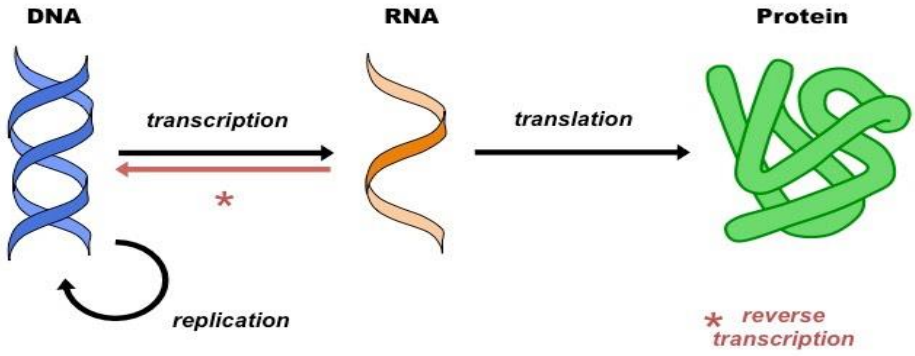

Fig. 1.1 The central dogma of Molecular Biology (https://ib.bioninja.com.au/standard-level/topic-2-molecular-biology/27-dna-replication-transcri/central-dogma.html)

Fig. 1.2 Structure of an intrinsically disordered protein (IDP) depicting an ensemble of conformations adopted by an IDP. Adapted from Uversky, *J. Biol. Chem*., 2016, 291(13), 6681-6688. (Ref 40)

Our understanding of proteins is totally ingrained with the opinion that for a protein to function a well-defined three dimensional structure is a prerequisite condition. However, there are certain class of proteins which are natively unfolded or intrinsically disordered (IDP). 33% of eukaryotic genome is composed of IDPs and they can bind with multiple partners and hence adopt a wide range of structures upon binding [3,4]. In 2002, Peter Tompa reported many proteins and domains of proteins such as calpastatin, α-synuclein, non-amyloid β component of Alzheimer's disease (AD), microtubule associated protein Tau, transactivator domain (TAD) of transcription factor and many more, which do not have a folded structure but exhibit highly flexible and a random-coil-like conformation under physiological conditions. The fact that these IDPs are the native state of proteins which carry out a large number of important physiological functions led Dyson and Wright to propose that the classical protein structure-function paradigm needs to be re-assessed [5] . A huge number of papers, in past few years, have appeared on the proteins, which are denoted as intrinsically unstructured/disordered or natively denatured/unfolded such as α-synuclein, Tau, and play significant roles in regulation of cellular processes, replication, signalling etc.[6,7,8]. Several years of research has revealed that IDPs comprise of the following physico-chemical attributes such as low mean hydrophobicity, high net charge due to presence of hydrophilic amino acids like aspartic acid, glutamic acid, arginine and lysine which results in loss of hydrophobic character and increases the net charge and facilitates self-assembly. Owing to these characteristics, IDPs adopt an ensemble of conformations (Fig. 1.2) which range from being expanded to partially-expanded to collapsed structures that undergo continuous fluctuations and transitions. Such conformational plasticity of IDPs can lead to

uncontrolled self-assembly of IDPs under conducive solution conditions. For instance, IDPs are soluble and functional in their monomeric form but they can undergo a conformational transition into ordered, amyloid aggregates which are implicated in various neurodegenerative disorders such as Huntington's, Parkinson's and Alzheimer's disease etc.[9] One of such IDPs is Tau protein which is involved in the pathogenesis of Alzheimer's disease. Tau aggregates deposition is also detected in many other taupathies such as progressive supranuclear palsy (PSP), Pick's disease (PiD), corticobasal degeneration (CBD), Down's syndrome (DS), frontotemporal dementia [10]. The common connection between all the tauopathies, irrespective of all the mutations and post-translational modifications found on tau, is the aggregated form of tau [11]. In all these pathological diseases, it has been reported that the intrinsically disordered tau undergoes a conformational transition and self-assembly from monomeric random-coil to ordered polymeric cross β-sheet-rich fibrils known as amyloid fibrils. The amyloids were first observed more than 150 years ago in systemic amyloidosis, deposited in the organs and tissues of the patients. It is proposed that the soluble IDPs form protofibrillar structures that eventually lead to the formation of amyloid fibrils [12].

.

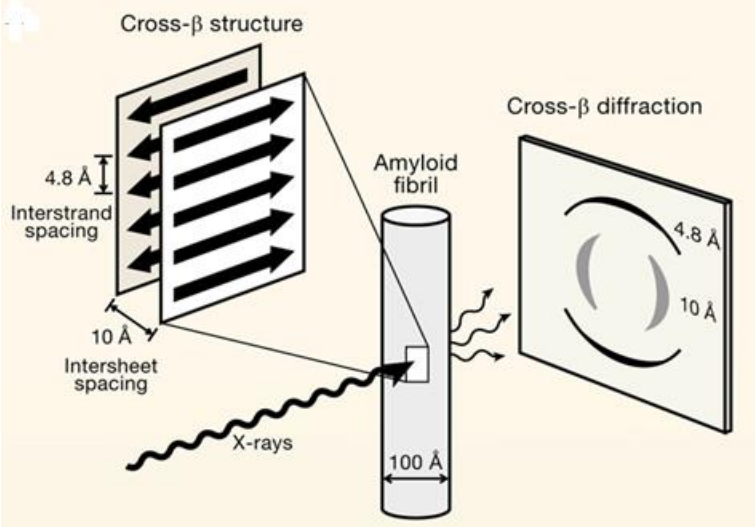

Fig. 1.3 The cross-β structure of an amyloid fibre elucidated using X-ray diffraction. Reprinted from Cell, 148, Eisenberg & Jucker, The Amyloid State of Proteins in Human Diseases, 1188-1203, Copyright (2012), with permission from Elsevier. (Ref 41)

The common biophysical definition of an amyloid fibril is that when examined with X-rays they display a cross-β diffraction pattern and it was first reported by William Astbury in 1935. With the help of cross β pattern, Astbury analysed that protein chains are present perpendicular to the fibrillar axis and assemble together into the sheets that are parallel to

each other. The model suggested that the protein strand responsible for the formation of β sheets can run in the alternate opposite directions forming anti parallel β sheets or in same direction forming parallel β sheets. Fig. 1.3 depicts the X-ray diffraction pattern of a cross β-sheet rich amyloid fibril. The X- ray diffraction confirms the presence of two characteristic diffuse reflections. One at the vertical axis at a spacing of 4.8 Å which arise from the stack of β-strand and the other most diffuse reflection along the horizontal axis at a spacing of approximately 10 Å which arise from the gap or separation between the adjacent β-sheets [14].

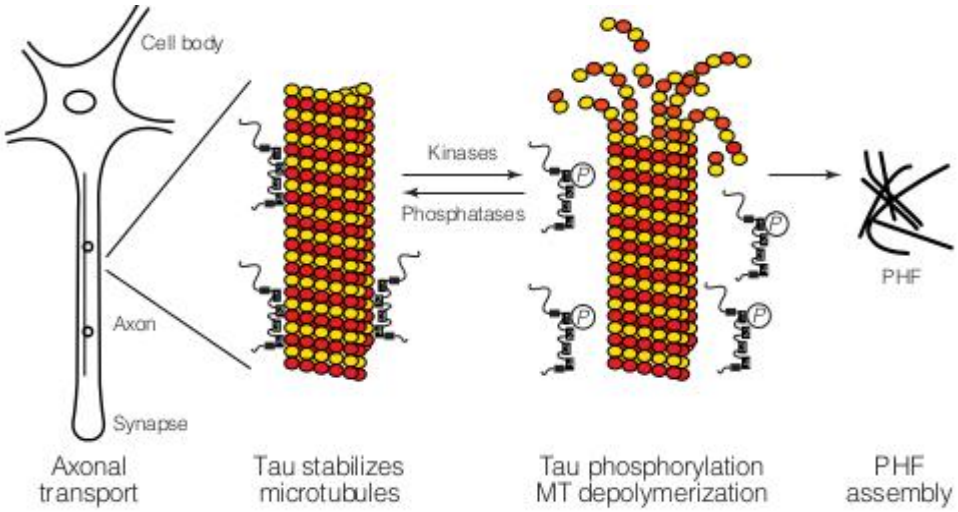

Fig. 1.4 Tau is mainly responsible for stabilization of neuronal microtubules. Abnormal tau (hyperphosphorylated) has weak affinity for microtubules and hence releases in the cytosol and responsible for destabilization of microtubules (http://neurowiki2014.wikidot.com/individual:molecular-mechanisms-of-pathology:possible-hypoth)

Tau is a 441-residue IDP which is primarily expressed in the central nervous system and is involved in the stabilization of microtubular cytoskeleton. The primary structure of Tau is classified into three distinct functional domains namely, (a) the N-terminal domain (residues 1 - 197) which is primarily acidic (~120 residues) and contains one proline-rich domain (P1), (b) the central domain (residues 198 – 400) which contains another proline-rich domain (P2) and microtubule-binding repeat domains (R1-R4) that are predominantly basic and (c) the C-terminal domain (residues 401 - 441) which is largely neutral. Based on Tau's phosphorylated forms, it binds to the microtubules through MT (microtubule) binding region. However, besides carrying out important physiological functions, Tau is also involved in Alzheimer's diseases as mentioned earlier. For instance, it has been documented that during amyloid assembly, Tau changes into its abnormal form i.e. hyper phosphorylated form, which

destabilizes the microtubules as the hyper phosphorylated form weakens its affinity towards the microtubule and hence tau releases in the cytosol regions and causes MT disassembly (Fig. 1.4). These hyperphosphorylated forms of Tau forms amyloid aggregates and changes into the pathogenic inclusions known as paired helical filaments (PHFs) which further convert into more aggregated form i.e. Neuro fibrillary tangles (NFTs). These NFTs deposit in the tissues and cells of brain and destroys the neurons and hence causes pathological problems. Elucidating the molecular mechanism of these protein self-assembly processes is of paramount importance both in terms of gaining fundamental knowledge and also in terms of drug design and clinical intervention.

In this thesis, we have investigated the molecular mechanism of TauK18 aggregation using SDS as the anionic inducer because it is a well-known lipid-mimetic. Efforts were directed towards delineating the early key steps towards TauK18 amyloid assembly. Several spectroscopic techniques such as fluorescence, circular dichroism in addition to biochemical techniques were used to decipher the aggregation kinetics and the morphological transitions were monitored using atomic force microscopy (AFM). All the results and discussions are described in chapter 4 of this thesis.

CHAPTER 2

Literature Review

Weingarten et al., 1975 reported Tau as a neuronal protein which is associated to microtubules (MTs) in porcine brain and known as a microtubule-associated protein. The biochemical studies on Tau revealed that Tau was sufficient for both extension and nucleation of microtubules [17]. Tau protein plays a very significant role in microtubule assembly and dynamics that helps in regulation of neuron morphology [18]. Because of its intrinsically disordered structure Tau is an acid and heat stable protein. In the brain of adult humans, a single gene located on chromosome number 17 known as mapt, is responsible for encoding of Tau protein [19]. This gene yields six different isoforms, after its transcription into a nuclear RNA, containing or lacking exons 2, 3, and 10 by alternative splicing [20]. In the N-terminus of Tau (called N),exon 2 and exon 3 encodes for 29 amino acids stretch and based on this Tau isoforms can be of three types, 0 N (neither of them), 1N (one insert, exon 2 only), and 2 N (both inserts) (Fig.2.1a). In the C-terminus exon-10 encodes for 31-amino acid, form a microtubule-binding repeat called R and based on this Tau isoforms can have 3 repeats (3R, exon 10 not included) and 4 repeats (4R, exon 10 included) [21,22]. Hence, based on this 6 different isoforms of proteins are possible, whose length varies from 352-441 residues. When analysed on SDS PAGE, these different isoforms migrates as a set of six different bands with molecular masses ranges from 48-67 kDa [23].

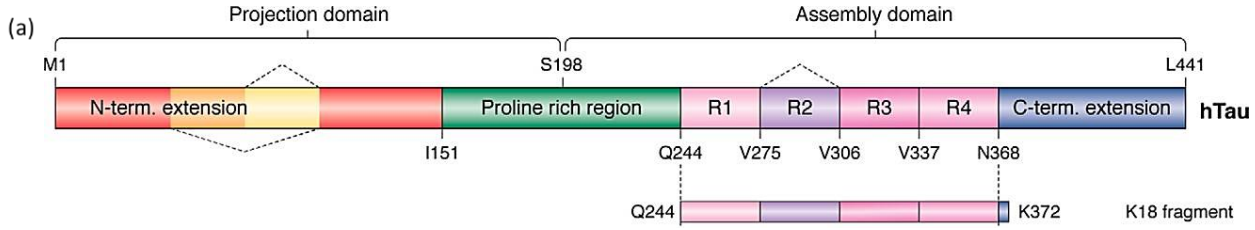

(b)

Tau K18

244	QTAPVPMPDL	**K**NV**K**S**K**IGST	ENL**K**HQPGGG	**K**	274 R1
275	**KK**LDLVQIIN	SNVQS**K**CGS**K**	DNI**K**HVPGGG	S	305 R2
306	VQIVY**K**PVDL	S**K**VTS**K**CGSL	GNIHH**K**PGGG	Q	336 R3
337	VEV**K**SE**K**LDF	**K**DRVQS**K**IGS	LDNITHVPGG	GN	368 R4
369	**KK**IE				372

Fig. 2.1 A schematic representation of **(a)** Different domains of longest isoform of Human Tau protein. Adapted from Lippens et al., *J. Biol. Chem*., **2019**, *294*, 9316-9325. (Ref 42) **(b)** Amino acid sequence of Tau K18 wherein lysines are shown in blue color. Adapted from Bhasne et al*., J. Mol. Biol*., **2018**, *430*, 2508-2520. (Ref 37)

Tau is a highly soluble protein whose overall amino acid composition is hydrophilic, as estimated for an IDP (Fig 2.1b). The approximately 40 amino acid residues at C terminal are neutral and approximately 120 amino acid at N terminal are acidic (based on 2N4R, the longest isoform of Tau). Amino acid residues from 151-243 are proline rich and hence are basic and known as P1 and P2 domains. Depending on the isoform the repeat domain regions can be made of 3R or 4R. When digested in vitro with chymotrypsin, it gets cleaved after tyrosine 197. This cleavage gave rise to two domains, the C-terminal and the N- terminal domain. The N- terminal domain consist of amino acid residues from 1 to 197 and it is known as the 'projection domain' because on digestion it is projected away from the MT surface. The C-terminal domain consist of amino acid residues from 198-441 and it is known as the assembly domain because it binds with the MT regions and promoted their assembly [24,25]. NMR (Nuclear Magnetic Resonance) studies of Tau explained three domains.1) The projection domain (1-197), 2) The central domain (198-400) and 3) The C-terminal domain (401-441). The Tau K18 fragment in consist of 4 repeats regions of full length Tau [26]. The four repeat regions are known as R1, R2, R3, and R4.

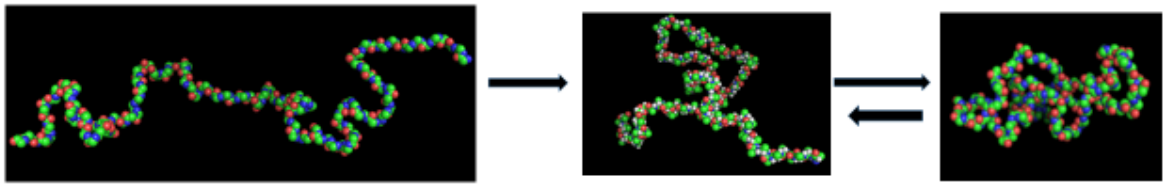

Fig. 2.2 Different conformations of TauK18 namely, **(a)** Expanded form **(b)** Partially-collapsed form **(c)** Fully-collapsed form. Generated from PeDB 6AAC by using PyMOL (Schrodinger LLC).

Tau can exists in different conformations namely, an expanded form, partially-collapsed form and a fully-collapsed form (Fig. 2.2). All of these three conformers exist in equilibrium but the equilibrium is shifted more towards the fully collapsed form and hence it preferentially favours the fully collapsed form over the other forms because of stronger chain-chain interactions compared to chain-solvent interactions. As stated earlier, it is an intrinsically disordered protein and does not possess any proper secondary and tertiary structure as studied by different techniques like FTIR (Fourier transform infrared spectroscopy), CD (circular dichroism), electron microscopy or small angle X-ray scattering (SAXS). Most recent studies of full length tau and of the repeats domain are being done with the help of NMR (nuclear magnetic resonance) and SAXS (small angle X-ray scattering). The NMR studies have shown

the presence of transient secondary structure (β-strand, α-helix). The two C-terminal tail and N- terminus possess two stretches of α-helical and the beginning of R2-R4 repeats have shown the presence of β-structure [27].

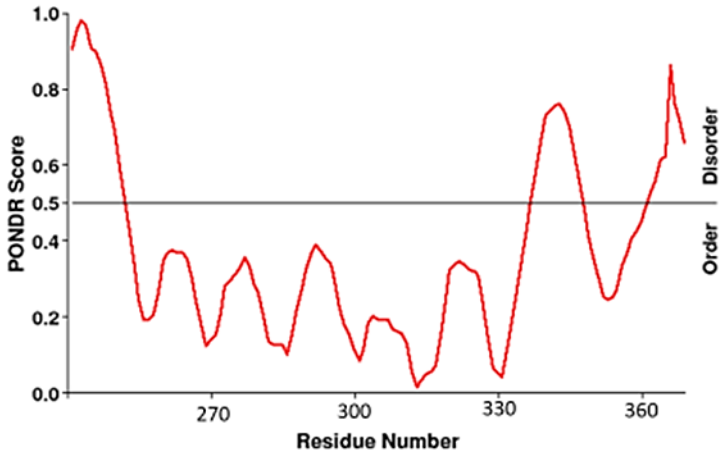

Fig. 2.3 Pondr plot predicting disorder in the Tau K18 sequence generated using http://www.pondr.com/

Fig. 2.3 shows the randomness in the structure of Tau K18. Residue number 244 to 372 of full length Tau forms the Tau K18. The amino acid residues numbered from ~255 to 330 and from ~345-360 form an ordered structure whereas residue numbers ~244-254 and ~331-344 form the disordered structure.

In addition to carrying out important physiological functions, Tau is also implicated in detrimental Alzheimer's disease. Alzheimer's disease (AD) is characterized by the presence of two structures in the brain: 1) Intracellular neurofibrillary tangles (NFTs) and 2) extracellular senile plaque. The neurofibrillary tangles (NFTs) are the aggregates formed by the hyper phosphorylated forms of the Tau protein and the senile plaques are the aggregates formed by the amyloid β (Aβ) protein. All the forms of protein Tau are responsible for the formation of NFTs. Tau aggregation and Alzheimer's disease (AD) has strong connection because the location and number of NFTs are directly linked with the decline and degree of severity of the Alzheimer's disease [11]. The main reason of the tauopathies including Alzheimer's irrespective of the modifications and mutation found in the protein Tau, is the tau aggregation. In the tauopathies, the disordered and monomeric Tau get converted into

ordered protein supramolecular aggregates known as amyloid fibrils. Typically, Tau amyloid fibril formation follows a nucleation dependent polymerization mechanism (Fig. 2.4). The nucleation dependent polymerization mechanism of amyloid aggregation has 3 significant characteristics: 1) a S-shaped sigmoidal growth curve composed of three phases (lag phase, log/growth phase and a saturation phase), 2) a critical concentration, this is the concentration below which fibril assembly is not possible and 3) the elimination of the lag phase by the help of addition of the seeds (preformed fibrils) [28]. For an aggregation mechanism to be considered as nucleation dependent process until all above three mentioned criteria are completed. Tau amyloid fibrils are known to form straight filament (SF) and paired helical filaments (PHF). The PHFs are made up of a twisted double helical fibril, the length of cross repeat of fibril is approximately 80 nm and width varying between 8 and 20 nm and the straight filaments have a width of approximately 15 nm [29].

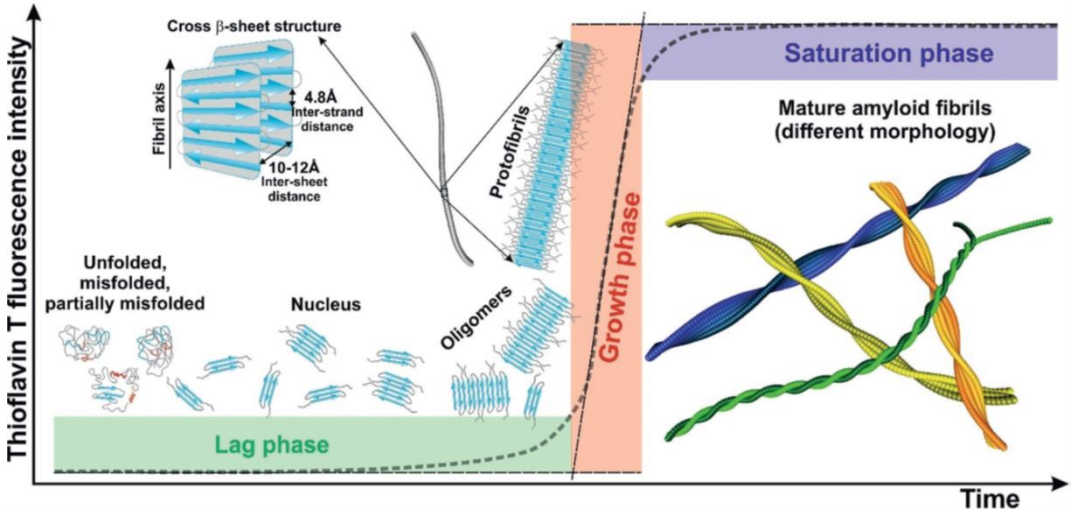

Fig.2.4 Schematic representation of amyloid aggregation kinetics of unfolded peptide chains into amyloid fibrils which shows a sigmoidal growth comprising lag phase, growth phase and saturation phase. Reprinted from Angew. Chem. Int, Ed, 57, Adamcik & Mezzenga, Amyloid Polymorphism in the Protein Folding and Aggregation Energy Landscape, 8370-8382, Copyright (2018), with permission from John Wiley & Sons. (Ref 43)

Several studies on mechanism of formation of tau fibril *in vitro* have indicated that the microtubule-binding repeat domain of tau is responsible for the formation of amyloid fibril core and that is why several studies use the repeat domain as the model protein to investigate tau aggregation [11]. To initiate the aggregation of tau *in vitro*, an inducer is required because tau protein does not form fibrils spontaneously at physiological concentration of protein (1-10 μM) even under the buffer conditions of high or low pH, while other fibril forming proteins including α-synuclein do not require such inducers. Unlike α-synuclein, tau does not form

amyloid fibrils spontaneously at physiological concentrations of protein even at extremes conditions of temperature and pH because tau protein does not have enough mean hydrophobicity required to form a collapsed structure under these buffer condition. One study on full length tau protein has shown that without the presence of an inducer, 8 µM concentration of protein took 8 months in 100 mM NaCl (pH 7) buffer and 10 mM HEPES. Whereas, in the presence of an inducer, tau has shown aggregation in the reasonable time period of days at physiological concentrations only. Some of the inducers used for tau aggregation reactions are the compounds such as taurine, Quinone, urea, hexafluro-2-propanol and sulphated glycosaminoglycan like fatty acids, heparin, detergents, RNA, vesicles and lipids [30-35]. Most of these inducers are anions like RNA and heparin are negatively charged polymers. Goedert in 1996 reported that heparin prevents the binding of tau to microtubules and hence encouraged disassembly of microtubules. It has been suggested in previous literature reports that Tau requires a negatively charged surface of sulfonate, carboxylate and an alkyl chain of at least 12 carbon atoms for fibrillization [32]. The detergents and fatty acids form negatively charged micelles above the CMC to work as the inducers. It has found that the negatively charged surface provided by the inducers results in stabilization of the aggregation-competent conformations of the protein tau and helps in raising the local concentration of protein tau and as a results helps to overcome the energy barrier for aggregation. These studies proposed that anionic surfaces nucleate fibrillization of tau *in vitro* and based on these observations, it was concluded that anionic membrane can induce tau fibrillization *in vivo*. However, it has been observed that higher concentrations of inducer can also result in inhibition of the aggregation. The higher concentration of heparin that surpassed the dissociation constant for the generation of the on-pathway intermediate results in reduction in the relative stability of the aggregation competent dimer. Different temperature and pH values also effect the aggregation mechanism. Additionally, Seidler in 2017 reported that VQIINK sequence of tau present in the repeat region of tau is majorly responsible for the aggregation of tau [36]. Engineered tau prepared by the biochemists containing only the VQIINK sequence aggregated much faster than the wild-type (WT) strain. Several studies on amyloid fibril formation have shown the existence of structural heterogeneity with difference in internal structure or external morphology under same and different aggregation condition. However, the molecular mechanism of TauK18 amyloid aggregation along with detection of early key steps still remain elusive. In addition to these reports, some proofs for structural heterogeneity in fibril of tau also exists, as measured by solid state nuclear magnetic resonance (ssNMR) and electron paramagnetic resonance (EPR) spectroscopy [11]. The results

of above mentioned techniques have revealed that fibril polymorphs arise from the use of different kinetic pathways for protein aggregation, but there are no direct evidences for this hypothesis. Identifying the kinetic origin of heterogeneity in structure of fibril of tau is a challenging and important aim of mechanistic study that are regulated towards the intelligent design of drugs and inhibitors.

Hence, in this thesis, we have investigated the molecular mechanism of TauK18 aggregation using SDS as the anionic inducer because it is a well-known lipid-mimetic. Efforts were directed towards delineating the early key steps towards TauK18 amyloid assembly. Several spectroscopic techniques such as fluorescence, circular dichroism in addition to biochemical techniques were used to decipher the aggregation kinetics and the morphological transitions were monitored using atomic force microscopy (AFM). All the results and discussions are described in chapter 4 of this thesis.

CHAPTER 3

Materials and Methods

3.1 Reagents

The protein namely, TauK18, was recombinantly expressed and purified from bacterial culture. The materials for bacterial culture and protein expression such as Luria Broth was procured from HiMedia, antibiotics such as chloramphenicol and ampicillin were obtained from GoldBio and MP Biomedicals, respectively. IPTG (Isopropyl β-D-1-thiogalactopyranoside) was obtained from BR Biochem. All the other chemicals such as ThT (Thioflavin-T), ANS (8-anilinonaphthalene-1-sulphonic acid), SDS (sodium dodecyl sulfate), glutaraldehyde, acrylamide, bis-acrylamide, coomassie blue, and materials for buffer preparations such as MES (2-(N-morpholino) ethanesulphonic acid), EDTA (ethylenediaminetetraacetic acid), DTT (dithiothreitol), sodium phosphate monobasic dihydrate were procured from Sigma Aldrich as the highest purity grade and used as obtained.

3.2 Glassware and labware used

Micropipettes (Eppendorf Research), micropipette tips, SP Sepharose column, SDS-PAGE apparatus, microcentrifuge tubes, cuvettes (for recording fluorescence spectra and anisotropy 10×10 mm, 10 mm × 2 mm cuvettes were used whereas for recording Circular Dichroism (CD) spectra, 10×1 mm cuvette was used, microtiter plate, reagent bottles, kim wipes.

3.3 Equipments and Instruments used in this study

3.3.1. Magnetic stirrer with hot plate

The magnetic stirrer is a device used to generate magnetic field which is responsible for the rotation of magnetic stir bar kept inside our sample and the sample is placed on the hot plate that heats up our sample. In this study the magnetic stirrer IKA RCT Basic was used. Its maximum speed is 1800 rpm and maximum temperature to which it can go is 310 ^{o}C. For our experiments, following parameters were used: Temperature: 37 °C and stirring speed: 800 rpm.

3.3.2. Fluorescence spectrophotometer

Fluorescence spectrophotometer is broadly used to investigate several processes in biology and chemistry including the interactions of the solvent molecules with the fluorophores, the rotational diffusion of the biomolecules and the distances between the sites on the biomolecules, their conformational changes and the binding interactions. The usefulness of the fluorescence is expanded by advances in the technology for processes like single molecule detection and cellular imaging [38]. For my thesis, the fluorescence emission intensity and fluorescence anisotropy were measured on Perkin Elmer Fluorimeter and Fluoromax-4 (Horiba Jobin Yvon, NJ) fluorimeter, respectively to investigate the mechanism of Tau K18 amyloid assembly using anionic inducer (SDS). Proteins show fluorescence due to the presence of aromatic amino acids namely, tryptophan, tyrosine and phenylalanine which exhibit a change in the fluorescence intensities due to changes in the protein structures. Tau K18 contains only one tyrosine which is the basis of the intrinsic fluorescence. Additionally, ThT is an amyloid indicator which is used to monitor the amyloid aggregation reaction of a protein. It shows a strong fluorescence signal upon binding with the amyloids. In this work, an extrinsic fluorophore i.e. ANS (1,8-anilonapthalene sulfonic acid) was also used which reports on changes in the hydrophobic environment within the protein and/or protein aggregates as a result of amyloid assembly. ANS shows very weak or negligible fluorescence at 505 – 510 nm in aqueous solution but its fluorescence intensity increases significantly with a simultaneous blue-shift to ~475 nm when it binds to hydrophobic core.

3.3.3. Circular Dichroism (CD) spectrophotometer

Circular Dichroism (CD) is a spectroscopic technique which is used to study the secondary and tertiary structure of proteins. In this study the changes in the protein structure were analysed during its aggregation using Chirascan CD Spectrophotometer (Applied Photophysics, UK). In CD, a plane polarised light which is sum of two circularly polarised light of equal magnitude (one rotates clockwise, known as right circularly polarised light and the other rotates counter clockwise, known as left circularly polarised light) is allowed to pass through an optically active compound. The absorbance of RCP (A_R) is different from the absorbance of LCP (A_L) and this absorbance difference is the basis of study of CD. The electric field radii vector for one of the components changes after they are made to pass through the optically active sample as the sample preferentially absorbs one of the circularly polarized light over the other and hence the combination of these two vectors results in an

elliptically polarised light. In this work, the changes in the secondary structure of protein Tau K18 during amyloid assembly were recorded in the far-UV range (200 – 250 nm).

3.3.4. Plate Reader

The plate reader is an instrument which is used to monitor reactions with the help of microtiter plates. It is very useful because the microtiter plate contains 96 wells and hence, we can study 96 samples simultaneously. Also, it requires very less amount of sample (~160 μL) in each well. The plate reader used in this research work is POLARstar Omega (BMG LABTECH) which was used to monitor aggregation kinetics of Tau K18 using ThT fluorescence for longer periods of time.

3.4. Methodologies

3.4.1. Protein expression and purification

In this research, we expressed and purified Tau K18 using a literature protocol which is described briefly [37]. Typically, Tau K18 was cloned in pET23a vector and expressed in *Escherichia coli* BL21 (DE3) cells by using recombinant DNA technology. First the primary culture was grown in LB media containing the antibiotics (chloramphenicol (35 μg/mL) and ampicillin (100 μg/mL)) at 37 ^{o}C and 220 rpm in the shaking incubator for overnight. Then, the secondary culture was grown from the primary culture, 10 mL of primary culture is used for growing 1000 mL of secondary culture so as to maintain the ratio of 1:100 and was kept in the shaking incubator at 37 ^{o}C and 220 rpm. The optical density (OD) of the culture at 600 nm was checked at regular time intervals and when it reached an OD of 0.6, the culture was induced with 1 mM IPTG (Isopropyl β-D-1-thiogalactopyranoside) and kept in the shaking incubator at 37 ^{o}C and 220 rpm for 4 hours. The pellet was harvested by centrifugation at 4000 rpm for 30 min at 4 ^{o}C. The pellet was resuspended in the LB media and again centrifuged at 7000 rpm for 20 min at 4 ^{o}C. The cells were lysed by using lysis buffer, pH 8 (50 mM Tris, 10 mM EDTA, 150 mM NaCl) and then boiled at 100 ^{o}C for 30 minutes. The centrifugation of the lysate was done at 11500 rpm for 30 minutes at 4 ^{o}C, after this 136 μL of 10% streptomycin sulphate and 226 μL of glacial acetic acid were added to the supernatant so as to precipitate the DNA, and again centrifuged at 11500 rpm for 30 minutes at 4 ^{o}C. The supernatant was collected and mixed with saturated ammonium sulphate and incubated for 2 hours at 4 ^{o}C with gentle mixing for salting out protein. This was centrifuged at 11500 rpm for 15 min at 4 ^{o}C and the protein pellet was washed with 100 mM ammonium acetate and

100% ethanol and centrifuged at 4000 rpm for 10 minutes at 4 ^{o}C and again the pellet was washed with 100% ethanol and then kept overnight for drying at 25 ^{o}C. The pellet was dissolved in Buffer A (20 mM MES, 2 mM DTT, 1mM EDTA, 1 mM $MgCl_2$ of pH 6.8 and it was purified using SP Sepharose column by FPLC (Fast Protein Liquid Chromatography). The column was washed with milli-Q water, then with 1 M NaOH to remove the previous proteins from the column, again washed with milli-Q water, and washed with 1 M NaCl. Buffer A was added slowly with the help of the pipette from the sides of the column, so as to avoid any disturbance in the resin. Left the column as it is for the elution of the buffer. Meanwhile the protein was filtered with a syringe filter of 0.22 μm. After elution of the buffer A from the column, the filtered protein sample was injected into the column. In starting the flow rate was kept low so that the protein have enough time to bind with the resin. Again the column was filled with buffer A. After its elution the column was eluted with buffer B of pH 6.8 (20 mM MES, 2 mM DTT, 1 mM EDTA, 1 mM $MgCl_2$, 500 mM NaCl. The protein fractions were collected as it eluted out of the column and the absorbance of the fractions were recorded at 280 nm. After this, all the fractions were pooled together and was dialysed overnight by using dialysis membrane and buffer A. Following the dialysis, the absorbance of the dialyzed protein sample was checked again at 280 nm. Additionally, SDS PAGE was run to assess the purity of the purified protein fractions whereby a 15% resolving gel was used. After ensuring the purity of the protein fractions, they were divided into aliquots of equal volumes and stored at -80 ^{o}C.

3.4.2. Preparation of stock solutions

All the buffers and solutions were prepared in milli-Q water. The stock concentrations of SDS and NaCl were 10 mM and 5 M, respectively and were diluted by addition of milli-Q water according to their concentrations in the experiments. ThT and ANS, at first, their stock solutions of concentration 10 mM (stored at -20 ^{o}C) were prepared. For the spectroscopic studies, sub-stocks of 1 mM (stored at 4 ^{o}C) were prepared in milli-Q water for both ThT and ANS by 10-fold dilution. For ThT and ANS, from 1 mM sub-stock, the dilution buffer of 11.11 μM was prepared in 50 mM monobasic phosphate buffer of pH 7 and pH 7.4 respectively, so as to make their final concentration 10 μM in our reaction mixtures by adding 450 μL of it to 50 μL of the aggregation reaction mixture. For plate reader experiments, ThT final concentration was made to 20 μM in our reaction mixtures by its suitable dilution from 1mM stock solution.

3.4.3. Preparation of Monobasic Phosphate Buffers

For monobasic phosphate buffer two stocks of 500 mM of pH 7 and 7.4 were prepared and those were further diluted by 10-fold dilution to prepare 50 mM buffer solutions. The pH of both the buffers were adjusted by the addition of either NaOH or HCl. The final pH of both the buffers was maintained in the range of ±0.01 at room temperature and were stored at 4 ^{o}C in the refrigerator.

3.4.4. Monomeric studies of Tau K18 (in the absence and in the presence of SDS)

The concentration of the stock of Tau K18 after purification was 338 μM and was stored at -20 ^{o}C. Different concentrations (5-100 μM) of Tau K18 were used in our study prepared by dilution of the stock (338 μM) with the addition of 50 mM monobasic phosphate buffer of pH: 7. For monomeric studies, 2 mL of reaction mixtures were prepared of different concentrations of Tau K18 and SDS. For Tau K18 the concentrations 5, 10, 20 and 50 μM were prepared by 67.6, 33.8, 16.9 and 6.76 fold dilution of the stock (338 μM) respectively in monobasic phosphate buffer pH: 7 at room temperature. And for SDS the concentrations were 100 μM, 200 μM, 500 μM, 1 mM, and 5 mM prepared by 10^2, 50, 20, 10 and 2 fold dilutions of the stock solution (10 mM) respectively. And 2 mL of these monomeric reaction mixtures were prepared in monobasic phosphate buffer of pH: 7. The spectroscopic studies of Tau K18 were carried out both in the absence and in the presence of SDS to check the change in the Tyrosine fluorescence intensity due to the anionic inducer (SDS) at different concentrations of Tau K18 and SDS at room temperature.

3.4.5. Setting up the aggregation reactions

Different aggregation reactions were set up to study the aggregation kinetics of Tau K18 by observing the changes in ThT fluorescence intensities, ANS fluorescence intensities and ANS anisotropy. Briefly, the aggregation reactions were carried out in a pre-cleaned glass vial which was kept in a water-bath at a temperature of 37 ^{o}C and stirred at 800 rpm. The volume of the reaction mixture was kept as 2 mL. Both the concentrations of the protein and SDS were varied such as Tau K18 (5 μM, 10 μM, 25 μM, 50 μM, 75 μM, 100 μM) and SDS (100 μM, 200 μM, 1 mM) were used. For monitoring TauK18 aggregation using ANS fluorescence, 50 μM of Tau and 1 mM SDS was used. Each of these reactions were at least carried out thrice. The aggregation reactions were prepared by addition of appropriate volume

of Tau K18 and SDS in the monobasic phosphate buffer of pH 7 according to their concentrations. For the spectroscopic studies, aliquots of 50 μL were withdrawn from the aggregation reaction mixture at regular intervals which was diluted (10-fold) to a total volume of 500 μL using ThT or ANS containing dilution buffers. Additionally, plate reader-based experiments were also carried out whose details are mentioned below (section 3.4.6.b).

3.4.6.a. Steady-state fluorescence measurements

The steady state fluorescence measurements were carried out to investigate the changes in TauK18 structure both under monomeric and aggregated conditions. For all of these experiments, monobasic phosphate buffer of pH 7, 50 mM was used. Typically, the changes in monomeric protein conformation were studied by monitoring the changes in Tyrosine fluorescence intensity using Perkin Elmer Fluorimeter (LS 55) in a 10 × 10 mm quartz cuvette at room temperature. Following parameters were used: excitation wavelength: 275 nm, emission range: 290-380 nm, excitation slit: 10 nm and emission slit: 10 nm, scan speed: 50 nm/min and number of accumulations were set to 1.

The changes in ANS fluorescence intensity and anisotropy during TauK18 aggregation were monitored as a function of time using a photon-counting fluorimeter namely, Fluoromax-4 (Horiba Jobin Yvon, NJ). The samples were taken in a quartz cuvette of 10 mm × 2 mm at room temperature. For ANS fluorescence intensity, following parameters were used: excitation wavelength: 350nm, emission wavelength: 475 nm, excitation slit: 3 nm and emission slit: 5 nm, averaged over 2 scans, integration time: 2 seconds. All the fluorescence spectra were plotted after subtracting the respective buffer baseline with the help of Origin 2019 software.

3.4.6.b. Plate Reader-based Fluorescence spectroscopic measurements

In order to monitor the SDS-induced aggregation kinetics of TauK18 for longer periods of time, plate reader-based fluorescence measurements were carried out. Typically, TauK18 aggregation was monitored by recording the changes in Thioflavin-T (ThT) fluorescence intensity as a function of time using a 96-well Nunc plate on a Plate Reader (POLARstar Omega, BMG LABTECH). For these experiments, various concentration of protein (5 – 100 μM), SDS (50 μM – 2 mM), and NaCl (25 – 500 mM) were used whereas the concentration of ThT was kept constant at 20 μM. The aggregation reaction was carried out at 37 ^{o}C and 600 rpm. Following parameters were used: excitation filter: 480 nm, emission filter 485 ± 12

nm, cycle time: 5 minutes, number of cycles: 250, and the gain was adjusted to 1%. At least 5 replicates were set for each reaction condition and the resultant data were plotted from at least 2 independent experiments and fitted using nucleation dependent polymerization model using Origin 2019 software.

3.4.7. Circular Dichroism (CD) spectroscopic measurements

All of the far-UV CD spectra were collected on Chirascan CD spectrophotometer (Applied Photophysics, UK) using a quartz cuvette of 10 x 1 mm pathlength at room temperature. For recording the secondary structure of TauK18 monomer, a concentration of 25 μM was used. For monitoring the changes in secondary structure during the course of SDS-induced aggregation, aliquots were withdrawn at regular time intervals and were diluted 2-fold into a dilution buffer in such a manner so that the SDS concentration remained constant at 1 mM. For all of these experiments, pH 7, 50 mM phosphate buffer was used. The parameters used for the far-UV CD experiments were λ (scan range): 200 - 260 nm, time per point: 0.5 sec, path length: 1 mm, step size: 1 mm, and averaged over 3 scans. All the spectra were corrected by subtracting respective buffer baseline and plotted with the help of Origin 2019 software.

3.4.8. Glutaraldehyde crosslinking assay

The glutaraldehyde crosslinking assay was carried out to characterize the TauK18 oligomers using a reported protocol [39]. Briefly, the native Tau K18 (25 μM) protein and SDS-induced TauK18 oligomers (25 μM Tau K18 + 1 mM SDS) formed at room temperature before the start of aggregation were treated with three different concentrations of glutaraldehyde (0.1%, 0.05%, 0.01%) for 15 minutes at room temperature. Following the incubation, all the protein samples were quenched by freshly prepared aqueous solution of 0.05 M sodium borohydride and left undisturbed for 15 minutes. The samples were then analysed with the help of SDS-PAGE (15%) followed by coomassie blue staining and destaining, and finally the gel was visualized on Bio-Rad gel documentation system.

Chapter 4

Results and Discussion

4.1 Analysis of purified Tau K18

Tau K18 was cloned in pET23a vector, expressed in *Escherichia coli* BL21(DE3) cells by using recombinant DNA technology and purified as described in Chapter 3 of this thesis. The purity of Tau K18 was assessed using SDS-PAGE. The purified protein showed a band at 15 kDa corresponding to its molecular weight and this is in agreement with previous reports [45].

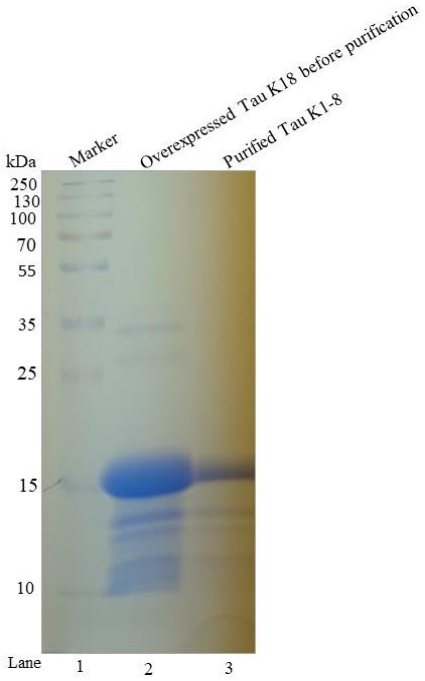

Fig. 4.1. SDS PAGE image showing bands for overexpressed Tau K18 before and after purification.

4.2 Effect of SDS on monomeric forms of Tau K18

Prior to investigating the amyloid aggregation mechanism of Tau K18, the protein was characterized under monomeric conditions to detect the presence of an amyloidogenic intermediate. Previous studies have indicated that Tau K18 forms amyloid aggregates in the presence of anionic inducers. Hence, a well-known lipid-mimetic namely, sodium dodecyl sulphate (SDS) was used as an anionic inducer to investigate the conformational changes in Tau K18 under monomeric conditions.

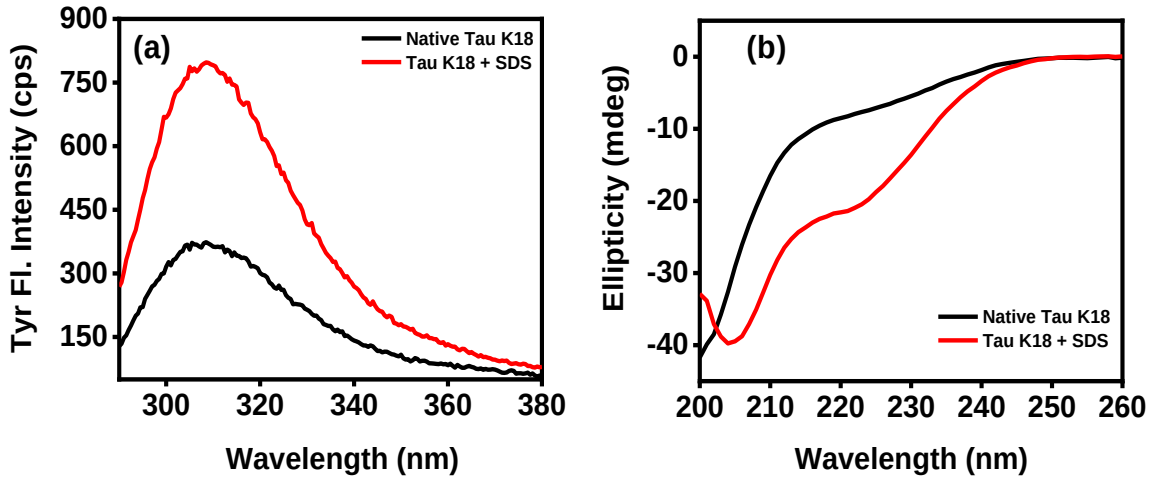

Fig. 4.2. (a) Tyrosine fluorescence spectra of 50 μM native Tau K18 only (black) and 50 μM of Tau K18 in the presence of 1 mM SDS (red) **(b)** Far-UV CD spectra of 25 μM Tau K18 in the absence (black) and in the presence of 1 mM SDS (red) showing a transition from random coil to α-helix after addition of 1 mM SDS.

Since Tau K18 is natively unfolded and contains a single tyrosine residue, the steady-state fluorescence emission of tyrosine was recorded. It was observed that the intrinsic tyrosine fluorescence showed an emission maximum at 310 nm. Upon addition of SDS, a significant increase in the emission intensity of tyrosine was observed which suggested that Tau K18 undergoes a conformational change whereby the lone tyrosine may get buried into a hydrophobic environment (Fig.4.2a). In order to confirm whether there is any significant conformational change in Tau K18 in the presence of SDS, the far UV CD spectra of the native protein in the absence as well as in the presence of SDS were recorded. It was observed that the intrinsically disordered Tau K18 shows a signature of random coil as expected and it undergoes a transition from random coil to a partial α-helix upon addition of SDS (Fig. 4.2b) which corroborates our tyrosine fluorescence data. Hence, taken together, our studies on monomeric Tau K18 suggested that it adopts a partially-folded α-helical structure instantaneously in the presence of SDS and we hypothesized that this intermediate might be an amyloid aggregation-competent species.

4.3 SDS-induced aggregation kinetics of Tau K18: Protein concentration dependence

In order to probe that whether the partially-folded α-helical structure of Tau K18 can indeed serve as an amyloidogenic precursor, we initiated SDS-induced Tau K18 aggregation kinetics studies at 50 μM protein concentration and a sub-micellar concentration of SDS of 1 mM.

The amyloid formation kinetics was monitored with the help of a well-known amyloid indicator namely, Thioflavin-T (ThT) by measuring the changes in its fluorescence intensity at 480 nm (Fig.4.3a). The ThT fluorescence intensity showed a gradual increase which suggested that the partially-folded α-helical structure of Tau K18 gradually transformed into cross β-sheet-rich amyloid fibrils and hence, confirming our hypothesis. Additionally, the SDS-induced aggregation reaction of Tau K18 showed a typical sigmoidal kinetics comprising of a lag phase, log phase and a saturation phase. In order to probe the minimal protein concentration required for triggering the amyloid assembly, the Tau K18 concentration was varied (5-100 μM) while keeping the SDS constant at sub-micellar concentration of 1 mM. It was observed that the amyloid assembly started only at 15 μM Tau K18 and very low concentrations of Tau K18 (5-10 μM) did not show any aggregation (Fig.4.3b). Moreover, the lag phase became progressively shorter with an increase in Tau K18 protein concentration whereby 75 μM depicted almost a negligible lag phase (Fig.4.3b)

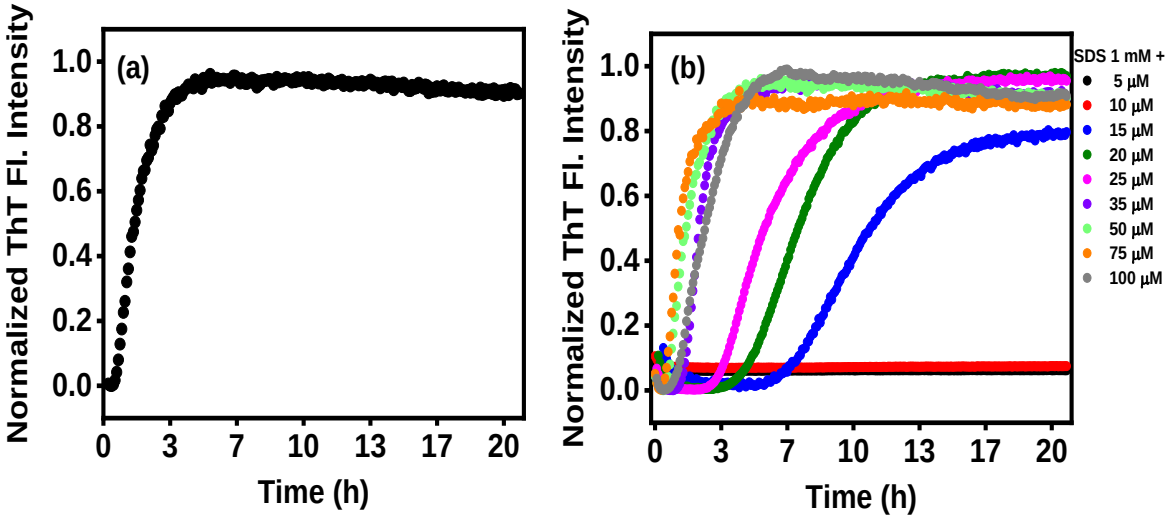

Fig. 4.3. Amyloid fibril formation kinetics of Tau K18, monitored by Thioflavin-T (ThT) fluorescence, in the presence of 1 mM SDS at 37 °C **(a)** A representative kinetics profile at 50 μM TauK18 **(b)** Variable concentration plot at Tau (5 -100 μM).

which implies that the aggregation proceeds via a nucleation-dependent polymerization mechanism. However, at 100 μM Tau K18, the lag phase was found to be slightly longer than that of 75 μM Tau and this phenomenon was observed repeatedly even in at least three independent experiments. This finding is in corroboration with a previous report on heparin-induced Tau K18 amyloid assembly [34]. Additionally, we would like to mention here that these aggregation reaction mixture of Tau K18 and SDS also became turbid as aggregation progressed. However, as expected, the lower concentration of the protein (5-10 μM) did not

show any turbidity because they did not form any amyloid aggregates within the timescale of our experiments.

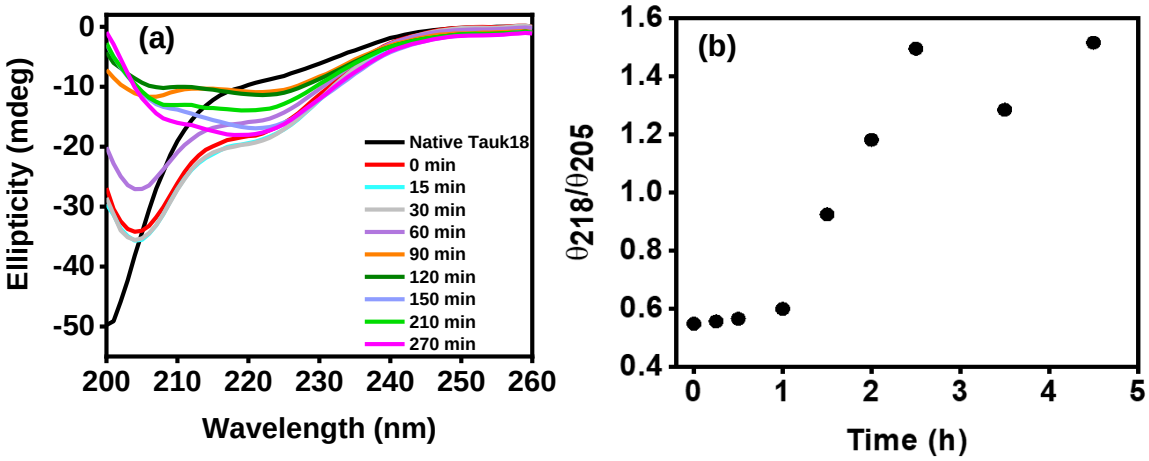

Fig. 4.4. Monitoring TauK18 aggregation kinetics in the presence of 1 mM SDS using far-UV CD spectroscopy **(a)** Far UV-CD spectra and **(b)** Ratiometric plot of ellipticities at 218 nm *vs* 205 nm.

4.4 Conformational changes of Tau K18 during amyloid assembly

As mentioned earlier (Fig. 4.2b), Tau K18 adopts a partially-folded α-helical structure instantaneously upon addition of SDS. Therefore, in order to characterize the conformational changes of Tau K18 during the course of aggregation, far-UV circular dichroism (CD) spectroscopic measurements were carried out. We observed that as amyloid aggregation progressed, Tau K18 showed a gradual conformational transition to a β-aggregated form, as expected for amyloids (Fig.4.4a). The figure also shows that the structural transition in the protein upon addition of SDS took place via an α-helical form and this form further gets converted into the β-aggregate. In order to assess the timescale of evolution of cross β-sheet-rich amyloids at the expense of random coils, a ratiometric plot of ellipticities at 218 nm *vs* 205 nm was obtained (Fig.4.4b). The ratiometric plot shows a sigmoidal kinetics wherein the lag phase contains the transient heterogeneous oligomeric species/nucleus comprising of both random coils and partial α-helices that eventually transform into β-sheet-rich amyloid aggregates as a function of time.

4.5 SDS concentration based aggregation kinetics of Tau K18: SDS and NaCl concentration dependence

Next, in order to find out the optimal concentration of SDS that is required for triggering the Tau K18 amyloid assembly, a concentration-dependent study was carried out whereby the SDS concentration was varied in the sub-micellar range (100-2000 μM) whereas the concentration of Tau K18 was kept constant at 50 μM (Fig.4.5a). It was observed that the lag phase decreased on increasing the concentration of SDS from 100 μM to 1000 μM, as expected, but showed a sudden increase in the presence of 2 mM SDS (Fig.4.5 (a)). This could be attributed to the fact that 2 mM SDS plausibly partially inhibits Tau K18 aggregation kinetics. Further analysis of the sigmoidal kinetics indicated that 100 μM SDS showed a lag phase of ~3 hours which became shorter with an increase in SDS concentration and finally negligible at 1 mM SDS. However, upon increasing the SDS concentration further to 2 mM, the lag phase increased to ~10 hours which indicates a delay in the aggregation kinetics.

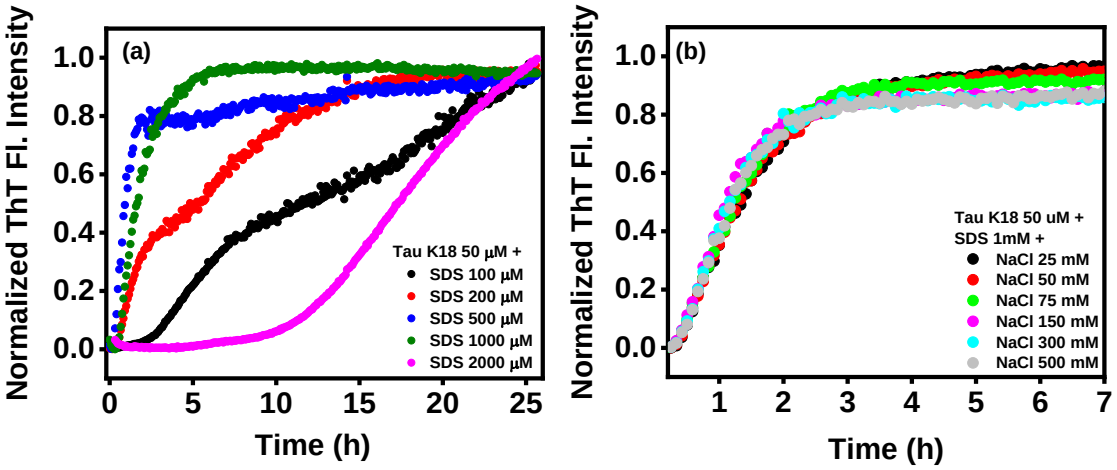

Fig. 4.5. Monitoring TauK18 aggregation kinetics by observing the changes in Thioflavin-T fluorescence in the presence of different concentrations of **(a)** SDS (100 - 2000 μM) **(b)** NaCl (25-500 mM).

Next, we conjectured that SDS-induced Tau K18 aggregation is mediated primarily by electrostatic interactions since Tau K18 has an overall positive charge whereas SDS is a negatively charged surfactant. Therefore, addition of salt would modulate the aggregation kinetics owing to an increase in the ionic strength of the aggregation mixture. Therefore, we carried out aggregation reactions in the presence of sodium chloride (NaCl) in a

concentration-dependent manner (25 mM to 500 mM) whereby both the Tau K18 and SDS concentrations were kept constant at 50 μM and 1mM, respectively (Fig.4.5b). We observed a very negligible effect on the lag phase of the reaction. The NaCl concentration based aggregation reactions showed a little decrease in the intensity of ThT with an increase in the concentration of NaCl.

4.6 Characterization of early formed oligomers of Tau K18 with SDS

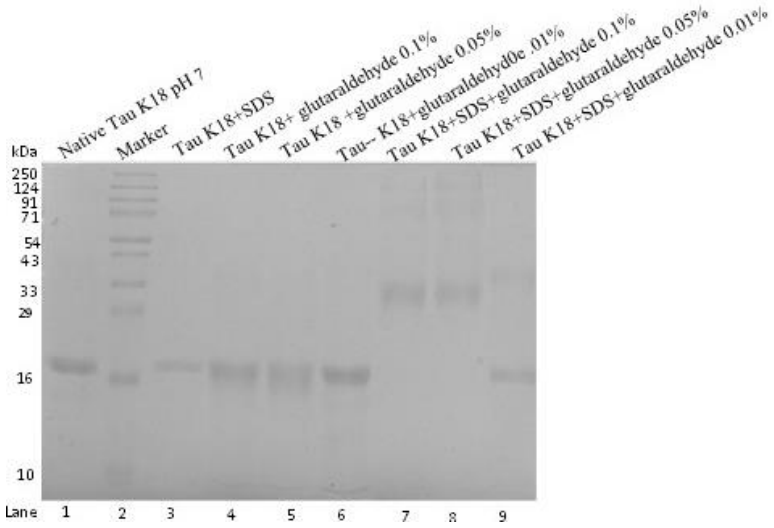

Fig. 4.6. Glutaraldehyde cross-linking assay of Tau K18 monomers and oligomers analysed on SDS-PAGE.

All of the aggregation assays which we have described earlier indicated that the initial intermolecular interactions between Tau K18 and SDS is critical which drives the amyloid assembly forward. Hence, in order to characterize these early intermediates, we performed glutaraldehyde crosslinking assay. Glutaraldehyde is a homo-bifunctional reagent which specifically reacts with primary amine groups and formed inter and intra subunits covalent bonds [44]. We observed the presence of Tau K18 dimers of molecular weight ~31 kDa which were found to be predominantly populated species in addition to other oligomers of higher molecular weight (Fig.4.6). As expected, no higher molecular weight bands were shown by Tau K18 alone in the absence of SDS which shows that sub-micellar SDS, indeed, triggers the aggregation.

4.7 Morphological transitions during aggregation

In order to monitor the morphological transformations during the time-course of aggregation of Tau K18, we used atomic force microscopy (AFM). The AFM images showed the formation of spherical oligomers (Fig. 4.7a) upon immediate addition of SDS that gradually matured into amyloid fibrils (Fig.4.7b) with an average height of 10-12 nm.

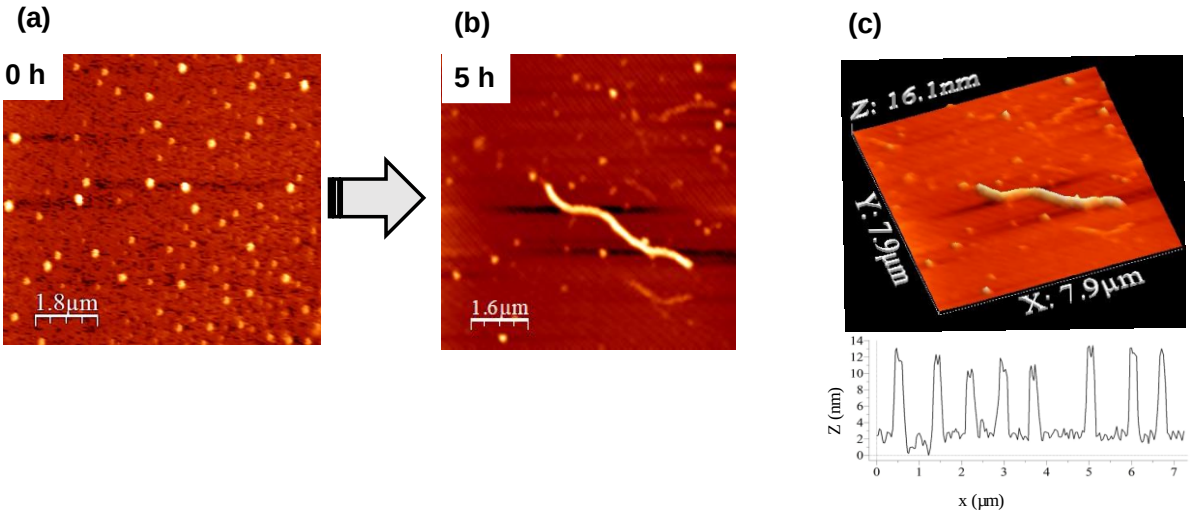

Fig. 4.7. AFM images of Tau K18 amyloid aggregates showing a morphological transition from **(a)** spherical oligomers at 0 hour of incubation to **(b)** an amyloid fibril after 5 hours of incubation **(c)** 3-D image of the same amyloid fiber along with its height profile.

CONCLUSION

This study provides insights into the amyloid aggregation mechanism of Tau K18 with the help of an anionic inducer using steady-state fluorescence and circular dichroism (CD) spectroscopic techniques. Our findings demonstrate that sub-micellar concentration of SDS was sufficient to trigger the amyloid assembly of Tau K18. We observed that the aggregation follows a sigmoidal growth kinetics and the lag phase shortens with an increasing concentration of protein and SDS that further indicates that the amyloid assembly proceeds via a nucleation-dependent polymerization mechanism. However, very high concentrations of both protein and SDS showed a slightly elongated lag phase repetitively and more experiments are underway to elucidate the mechanistic details of this phenomenon. An investigation into the conformational changes during Tau K18 amyloid aggregation revealed that the formation of a partially α-helical structure seems to be an obligatory intermediate during the initial time-points which eventually drives the formation of cross β-sheet-rich amyloid fibrils.

REFERENCES

1. Dobson, C. M. Principles of protein folding, misfolding and aggregation. *Seminars in Cell and Developmental Biology* **2004**, *15*, 3-16.
2. Vetri, V.; Librizzi, F.; Leone, M.; & Militello, V. Thermal aggregation of bovine serum albumin at different pH: comparison with human serum albumin. *European Biophysics Journal* **2007**, *36*, 717-725.
3. Tompa, P. Intrinsically unstructured proteins. *Trends in Biochemical Sciences* **2002**, *27*, 527-533.
4. Balcerak, A., Trebinska-Stryjewska, A., Konopinski, R., Wakula, M., & Grzybowska, E. A. RNA–protein interactions: disorder, moonlighting and junk contribute to eukaryotic complexity. *Open Biology* **2019**, *9*, 190096.
5. Wright, P. E.; & Dyson, H. J. Intrinsically unstructured proteins: re-assessing the protein structure-function paradigm. *Journal of Molecular Biology* **1999**, *293*, 321-331.
6. Csizmok, V.; Follis, A. V.; Kriwacki, R. W.; & Forman-Kay, J. D. Dynamic protein interaction networks and new structural paradigms in signalling. *Chemical Reviews* **2016**, *116*, 6424-6462.
7. Choi, U. B.; Sanabria, H.; Smirnova, T.; Bowen, M. E.; & Weninger, K. R. Spontaneous switching among conformational ensembles in intrinsically disordered proteins. *Biomolecules* **2019**, *9*, 114-129.
8. Wright, P. E.; & Dyson, H. J. Intrinsically disordered proteins in cellular signalling and regulation. *Nature Reviews in Molecular and Cell Biology* **2015**, *16*, 18-29.
9. Tipping, K. W.; van Oosten-Hawle, P.; Hewitt, E. W.; & Radford, S. E. Amyloid fibres: inert end-stage aggregates or key players in disease?. *Trends in Biochemical Sciences* **2015**, *40*, 719-727.
10. Nizynski, B.; Dzwolak, W.; & Nieznanski, K. Amyloidogenesis of Tau protein. *Protein Science* **2017**, 26, 2126-2150.
11. Ramachandran, G.; & Udgaonkar, J. B. Mechanistic studies unravel the complexity inherent in tau aggregation leading to Alzheimer's disease and the tauopathies. *Biochemistry* **2013**, *52*, 4107-4126.

12. Dunker, A. K.; Brown, C. J.; Lawson, J. D.; Iakoucheva, L. M.; & Obradović, Z. Intrinsic disorder and protein function. *Biochemistry* **2002**, *41*, 6573-6582.
13. Knowles, T. P.; Vendruscolo, M.; & Dobson, C. M. The amyloid state and its association with protein misfolding diseases. *Nature Reviews Molecular Cell Biology* **2014**, *15*, 384-396.
14. Eisenberg, D. S.; & Sawaya, M. R. Structural studies of amyloid proteins at the molecular level. *Annual Reviews of Biochemistry* **2017**, *86*, 69-95.
15. Kontaxi, C.; Piccardo, P.; & Gill, A. C. Lysine-directed post-translational modifications of tau protein in Alzheimer's disease and related Tauopathies. *Frontiers in Molecular Biosciences* **2017**, *4*, 56, doi: 10.3389/fmolb.2017.00056.
16. Weingarten, M. D.; Lockwood, A. H.; Hwo, S. Y.; & Kirschner, M. W. A protein factor essential for microtubule assembly. *Proceedings of the National Academy of Sciences USA* **1975**, *72*, 1858-1862.
17. Cleveland, D. W.; Hwo, S. Y.; & Kirschner, M. W. Physical and chemical properties of purified tau factor and the role of tau in microtubule assembly. *Journal of Molecular Biology* **1977**, *116*, 227-247.
18. Panda, D.; Miller, H. P.; & Wilson, L. Rapid treadmilling of brain microtubules free of microtubule-associated proteins in vitro and its suppression by tau. *Proceedings of the National Academy of Sciences USA* **1999**, *96*, 12459-12464.
19. Neve, R. L.; Harris, P.; Kosik, K. S.; Kurnit, D. M.; & Donlon, T. A. Identification of cDNA clones for the human microtubule-associated protein tau and chromosomal localization of the genes for tau and microtubule-associated protein 2. *Molecular Brain Research* **1986**, *1*, 271-280.
20. Avila, J.; Lucas, J. J.; Perez, M. A. R.; & Hernandez, F. Role of tau protein in both physiological and pathological conditions. *Physiological Reviews* **2004**, *84*, 361-384.
21. Lee, G.; Cowan, N.; & Kirschner, M. The primary structure and heterogeneity of tau protein from mouse brain. *Science* **1988**, *239*, 285-288.
22. Himmler, A. D. O. L. F.; Drechsel, D. A. V. I. D.; Kirschner, M. W.; & Martin, D. W. Tau consists of a set of proteins with repeated C-terminal microtubule-binding domains and variable N-terminal domains. *Molecular and Cellular Biology* **1989**, *9*, 1381-1388.

23. Goedert, M.; & Jakes, R. Expression of separate isoforms of human tau protein: correlation with the tau pattern in brain and effects on tubulin polymerization. *The EMBO Journal* **1990**, *9*, 4225-4230.
24. Steiner, B.; Mandelkow, E. M.; Biernat, J.; Gustke, N.; Meyer, H. E.; Schmidt, B.; & Kirschner, M. W. Phosphorylation of microtubule-associated protein tau: identification of the site for Ca2 (+)-calmodulin dependent kinase and relationship with tau phosphorylation in Alzheimer tangles. *The EMBO Journal* **1990**, *9*, 3539-3544.
25. Hirokawa, N.; Shiomura, Y.; & Okabe, S. Tau proteins: the molecular structure and mode of binding on microtubules. *The Journal of Cell Biology* **1988**, *107*, 1449-1459.
26. Mukrasch, M. D.; Bibow, S.; Korukottu, J.; Jeganathan, S.; Biernat, J.; Griesinger, C.;& Zweckstetter, M. Structural polymorphism of 441-residue tau at single residue resolution. *PLoS Biology* **2009**, *7*, e1000034.
27. Mylonas, E.; Hascher, A.; Bernado, P.; Blackledge, M.; Mandelkow, E.; & Svergun, D. I. Domain conformation of tau protein studied by solution small-angle X-ray scattering. *Biochemistry* **2008**, *47*, 10345-10353.
28. Frieden, C. Protein aggregation processes: in search of the mechanism. *Protein Science* **2007**, *16*, 2334-2344.
29. Crowther, R. A. Straight and paired helical filaments in Alzheimer disease have a common structural unit. *Proceedings of the National Academy of Sciences USA* **1991**, *88*, 2288-2292.
30. Goedert, M.; Jakes, R.; Spillantini, M. G.; Hasegawa, M.; Smith, M. J.; & Crowther, R. A. Assembly of microtubule-associated protein tau into Alzheimer-like filaments induced by sulphated glycosaminoglycans. *Nature* **1996**, *383*, 550-553.
31. Kampers, T.; Friedhoff, P.; Biernat, J.; Mandelkow, E. M.; & Mandelkow, E. RNA stimulates aggregation of microtubule-associated protein tau into Alzheimer-like paired helical filaments. *FEBS Letters* **1996**, *399*, 344-349.
32. Chirita, C. N.; Necula, M.; & Kuret, J. Anionic micelles and vesicles induce tau fibrillization in vitro. *Journal of Biological Chemistry* **2003**, *278*, 25644-25650.
33. Elbaum-Garfinkle, S.; Ramlall, T.; & Rhoades, E. (2010). The role of the lipid bilayer in tau aggregation. *Biophysical Journal* **2010**, *98*, 2722-2730.

34. Ramachandran, G.; & Udgaonkar, J. B. Understanding the kinetic roles of the inducer heparin and of rod-like protofibrils during amyloid fibril formation by Tau protein. *Journal of Biological Chemistry* **2011**, *286*, 38948-38959.
35. Barré, P.; & Eliezer, D. Structural transitions in tau k18 on micelle binding suggest a hierarchy in the efficacy of individual microtubule-binding repeats in filament nucleation. *Protein Science* **2013**, *22*, 1037-1048.
36. Seidler, P. M.; Boyer, D. R.; Rodriguez, J. A.; Sawaya, M. R.; Cascio, D.; Murray, K.; & Eisenberg, D. S. Structure-based inhibitors of tau aggregation. *Nature Chemistry* **2018**, *10*, 170-176.
37. Bhasne, K.; Sebastian, S.; Jain, N.; & Mukhopadhyay, S. Synergistic amyloid switch triggered by early heterotypic oligomerization of intrinsically disordered α-synuclein and tau. *Journal of Molecular Biology* **2018**, *430*, 2508-2520.
38. Lakowicz, J. R., Principles of Fluorescence Spectroscopy, (1999). Kluwer Academic/Plenum Publishers, New York.
39. Dalal, V.; Arya, S.; Bhattacharya, M.; & Mukhopadhyay, S. Conformational switching and nanoscale assembly of human prion protein into polymorphic amyloids via structurally labile oligomers. *Biochemistry* **2015**, *54*, 7505-7513.
40. Uversky, V. N. Dancing protein clouds: the strange biology and chaotic physics of intrinsically disordered proteins. *Journal of Biological Chemistry* **2016**, *291*, 6681-6688.
41. Eisenberg, D.; & Jucker, M. The amyloid state of proteins in human diseases. *Cell* **2012**, *148*, 1188-1203.
42. Lippens, G.; & Gigant, B. Elucidating Tau function and dysfunction in the era of cryo-EM. *Journal of Biological Chemistry* **2019**, *294*, 9316-9325.
43. Adamcik, J.; & Mezzenga, R. Amyloid polymorphism in the protein folding and aggregation energy landscape. *Angewandte Chemie International Edition* **2018**, *57*, 8370-8382.
44. Lindgren, M.; Sörgjerd, K.; & Hammarström, P. Detection and characterization of aggregates, prefibrillar amyloidogenic oligomers, and protofibrils using fluorescence spectroscopy. *Biophysical Journal* **2005**, *88*, 4200-4212.
45. Rametti, A.; Esclaire, F.; Yardin, C.; & Terro, F. Linking alterations in tau phosphorylation and cleavage during neuronal apoptosis. *Journal of Biological Chemistry* **2004**, *279*, 54518-54528.

Thesis-1

ORIGINALITY REPORT

14%	6%	9%	8%
SIMILARITY INDEX	INTERNET SOURCES	PUBLICATIONS	STUDENT PAPERS

PRIMARY SOURCES

1	Gayathri Ramachandran, Jayant B. Udgaonkar. "Mechanistic Studies Unravel the Complexity Inherent in Tau Aggregation Leading to Alzheimer's Disease and the Tauopathies", Biochemistry, 2013 Publication	2%
2	lism.cnrs-mrs.fr Internet Source	1%
3	Submitted to Higher Education Commission Pakistan Student Paper	1%
4	Submitted to Jawaharlal Nehru University (JNU) Student Paper	1%
5	Submitted to Indian Institute of Science Education and Research Student Paper	1%
6	d-nb.info Internet Source	1%
7	Shubhasis Haldar, Pallabi Sil, Muruganandan	<1%

Anjali Giri

06/09/19